Desalination and Water Treatment
www.deswater.com

doi: 10.5004/dwt.2022.28257

254 (2022) 15–24
April

Potassium hydroxide-treated walnut shell residue biochar for wastewater treatment: phenol adsorption and mechanism study

Jinyuan Zhang, Fengchuan Li, Shiping Zhou, Tao Li, Minghui Wu, Xianghong Li, Huijuan Li*

Key Laboratory of State Forestry and Grassland Administration on Highly-Efficient Utilization of Forestry Biomass Resources in Southwest China (Southwest Forestry University), Kunming 650224, China, emails: muzilihuijuan@163.com (H. Li), zjy961014@163.com (J. Zhang), 571875387@qq.com (F. Li), kmzhoushiping@163.com (S. Zhou), 2576561092@qq.com (T. Li), 2226747345@qq.com (M. Wu), xianghong-li@163.com (X. Li)

Received 15 June 2021; Accepted 21 January 2022

ABSTRACT

Using walnut shell as raw material and potassium hydroxide as an activating agent, the walnut shell carbon (denoted as WSC) was prepared for phenol adsorption. The prepared biocomposite adsorbent structure was investigated using N_2 adsorption–desorption analysis, Fourier-transform infrared spectroscopy, X-ray diffraction and scanning electron microscopy techniques. Adsorption efficiency of the prepared samples were investigated in various conditions such as activator ratio, initial phenol concentration, activation temperature, pH and adsorption reaction temperature. Also the kinetic and thermodynamic studies were carried out. The Brunauer–Emmett–Teller surface of the best WSC is 435.98 $m^2\ g^{-1}$ and the maximum pore volume is 0.299 $cm^3\ g^{-1}$, also it has a layered structure and porosity. When the mass ratio of WSC to KOH is 1:0.1, the amount of WSC (700°C, 2 h) is 2.0 g L^{-1} and the initial concentration of phenol is 20 mg L^{-1}, the adsorption properties show that the prepared WSC has good adsorption performance with the phenol removal rate of 98.78% in 60 min. The kinetic study illustrates that the phenol adsorption on WSC fits the non-linear pseudo-first-order. It indicates that the phenol adsorption on WSC is accompanied by mainly physical adsorption.

Keywords: Walnut shell carbon; Phenol; Adsorption; Kinetics properties

1. Introduction

Phenol-containing wastewater is a kind of industrial wastewater with great harm and wide range of pollution in the world, and it is an important source of water pollution in the environment [1–3]. Among them, phenol is a common pollutant in phenol-containing wastewater, and its removal has become the focus of attention in the field of water treatment. There are many techniques such as biological, adsorption, advanced oxidation technology, and also photocatalytic technology etc. [4–6]. Among these technologies, the adsorption technology has been used extensively for its simple operation and high efficiency. Today, biomass activated carbon has become a research hotspot due to its low price, wide sources and renewability [7–9]. Using pine fruit shell as a carbon source, Mohammed et al. [10] prepared biochar samples by slow pyrolysis and carried out for phenol biosorption onto these biochar, and thermodynamic parameters implied that the adsorption process was spontaneous and exothermic in nature. Ould-Idriss et al. [11] used olive wood to prepare activated carbon, and proposed that when the carbonization temperature of activated

* Corresponding author.

carbon chemically activated by H_3PO_4 rose above 450°C, a well-developed mesoporous phenomenon can be observed. Namasivayam and Sangeetha [12] modified coir pith activated carbon prepared by $ZnCl_2$ to remove phosphate from aqueous solution and suggested that the adsorption equilibrium data followed both Langmuir and Freundlich isotherms. Duranoğlu and Beker [13] used steam and KOH activation methods to prepare peach-stone-based activated carbons at 800°C, and showed that they had the highest surface area of 835 $m^2\ g^{-1}$ and micropore volume of 0.412 $cm^3\ g^{-1}$.

Walnut shell is widespread and fairly common in Yunnan Province of China, known as agro-waste biomass, has less commercial and nutrient values. However, walnut shell has high content of fixed carbon and volatile matter, and low ash content, which is suitable for preparing walnut shell carbon (WSC). Using walnut shells as raw material to prepare activated carbon can solve the problem of environmental pollution, and also can treat waste with waste [14–16]. Using Chinese walnut shell activated carbon as adsorbent, Yi et al. [17] studied Pb(II) adsorption from aqueous solution and showed that the amount of walnut shell charcoal was 2.0 g L^{-1}, the highest Pb(II) removal efficiency reached 94.12%. Zhao et al. [18] prepared activated carbon from walnut shells and studied the water vapor adsorption properties, and found that the highest water vapor adsorption capacity of the sample was 0.3824 g g^{-1}. Among the carbon activating agents, KOH is widely used as carbon activator, since it can play a major role in the improvement of specific surface area as well as porosity and hence increases the pollutants adsorption capability on the carbon materials

In this study, the activated carbon was prepared using walnut shells as raw materials and H_3PO_4, $ZnCl_2$ and KOH as chemical activators. The effects of activator ratio, calcination temperature, phenol concentration and pH value on the adsorption reaction were investigated. The prepared walnut shell activated carbon was characterized by X-ray diffraction (XRD), scanning electron microscopy (SEM), Brunauer–Emmett–Teller (BET) and Fourier-transform infrared spectroscopy (FTIR) techniques. The kinetic model and reaction mechanism of phenol adsorption on walnut shell activated carbon were proposed.

2. Materials and methods

2.1. Preparation of WSC

Walnut agricultural wastes were collected from agricultural market in Kunming, China. The walnut shell was washed thoroughly with distilled water to remove dust and other impurities. These were cut into small pieces with approximate size of 0.150 mm after removing dusts completely and dried in oven at 80°C for 12 h. The dried biomass was ground and then the powder biomass was carbonized at different temperature for 2 h under continuous nitrogen flow and the product obtained was labeled as walnut shell carbon (WSC). Then the activation of the waste shell was impregnated with chemical activator (KOH, H_3PO_4, $ZnCl_2$) by different biochar/activator weight ratios. The required amount of chemical activator was dissolved in 200 mL distilled water following the addition of raw waste shell and stirring for 6 h, then filtered and dried at 110°C for 24 h, calcined in a muffle furnace at different temperature for 2 h. The obtained WSC was thoroughly washed with distilled water until pH = 7.

2.2. Adsorption of phenol

To investigate the effect of adsorption efficiency with WSC, initial concentration of phenol, initial pH of the solution, and the adsorbent dose, the experiments were carried with a 100 mL phenol solution (the solvent is deionized water) with a concentration of 20 mg L^{-1}, added into an Erlenmeyer flask containing 0.2 g of WSC, and then place the Erlenmeyer flask in a constant temperature shaker in an incubator shaker (150 rpm) at constant temperature (25°C). Samples were taken at intervals of 10 min within 60 min. Taking 10 mL of the suspension and then centrifuge for 5 min at 5,000 rpm before phenol measurement. And the concentration was obtained by measuring the absorbance of supernatant at λ = 270 nm using a UV spectrophotometer (Pharo 300 Spectroquant, Merck, USA), which is consistent with the Lambert–Beer law. The degradation efficiencies of phenol were calculated using Eq. (1):

$$\text{Phenol conversion}(\%) = \frac{(C_0 - C_t)}{C_0} \times 100\% = \frac{(A_0 - A_t)}{A_0} \times 100\% \tag{1}$$

where C_0 and A_0 are the initial concentration and absorbance of phenol, also C_t and A_0 are the concentration and absorbance of phenol at a certain time, respectively.

2.3. Kinetics of phenol adsorption

The batch kinetics studies for phenol adsorption on WSC follow the same procedure as for the equilibrium studies. Samples were acquired at different times during the adsorption time to determine the concentrations (from 10 to 100 mg L^{-1}) of phenol as described above, experiments were performed using 0.2 g WSC in 100 mL phenol solution under the constant temperature shaker at 25°C. Samples are taken at intervals of 10 min. Take 10 mL of the suspension and centrifuge for 5 min in a centrifuge at 5,000 rpm, then picking 2.5 mL of the supernatant to measure the absorbance of the solution at λ_{max} = 270 nm with a UV spectrophotometer. The adsorption capacity was calculated using Eq. (2):

$$Q_e = \frac{(C_0 - C_e) \times V}{m} \tag{2}$$

where Q_e (mg g^{-1}) is the equilibrium adsorption capacity, C_0 is the initial concentration of phenol, C_e (mg L^{-1}) is the phenol equilibrium concentration, V (L) is the solution volume, and m (g) is the mass of WSC.

2.4. Characterization of photocatalysts

The X-ray diffraction (XRD) patterns were obtained by a horizontal Rigaku B/Max IIIB powder diffractometer

with Cu Kα (Kα = 0.15406 nm) radiation and a power of 40 kV at 30 mA. The morphology and structure of the samples were examined by JEOL/JSM-6335F scanning electron microscope (SEM). Surface characterization analyses were performed by N_2 adsorption at –196°C using Micromeritics TriStar 3000 instrument. BET surface areas (S_{BET}), micropore areas (S_{micro}), and total micropore volumes (V_{total}) were calculated from N_2 adsorption isotherms. And FTIR spectra (by Perkin-Elmer 1600 FTIR spectrophotometer) were obtained both before and after phenol adsorption of WSC.

3. Results and discussion

3.1. XRD analysis

Fig. 1a and b illustrate the XRD pattern for the five WSC obtained by different chemical activator and calcined at 700°C for 2h and WSC treated by KOH (1:0.1) calcined at different temperature. As can be seen in Fig. 1, the XRD pattern of WSCs shows a broad diffraction peak with 2θ values at 22.9° and 43.1° which can be attributed to graphitic (002) and (100) planes, respectively, which indicates that the WSC has been partially graphitized [19]. The obvious diffraction peaks at 2θ = 16.0° indicates the diffraction peaks of the amorphous body of hexagonal carbon caused by fatty chains. And when the WSC treated with ratio of 1:0.1 to KOH, the diffraction peak is more obvious. It may be caused by K vapor entering the microcrystalline layer at high temperature and catalytic oxidation reaction with carbon atoms that lead to lattice distortion or defect inside the graphite crystallite. From Fig. 1a it can be seen that the walnut shell treated by all chemical activator can form the graphitic (002) planes. However, untreated and KOH (1:0.1) treated have an obvious graphitic (110) planes, also the later obtained the best two planes of the graphitic planes, indicating that it can form the graphitic crystalline completely.

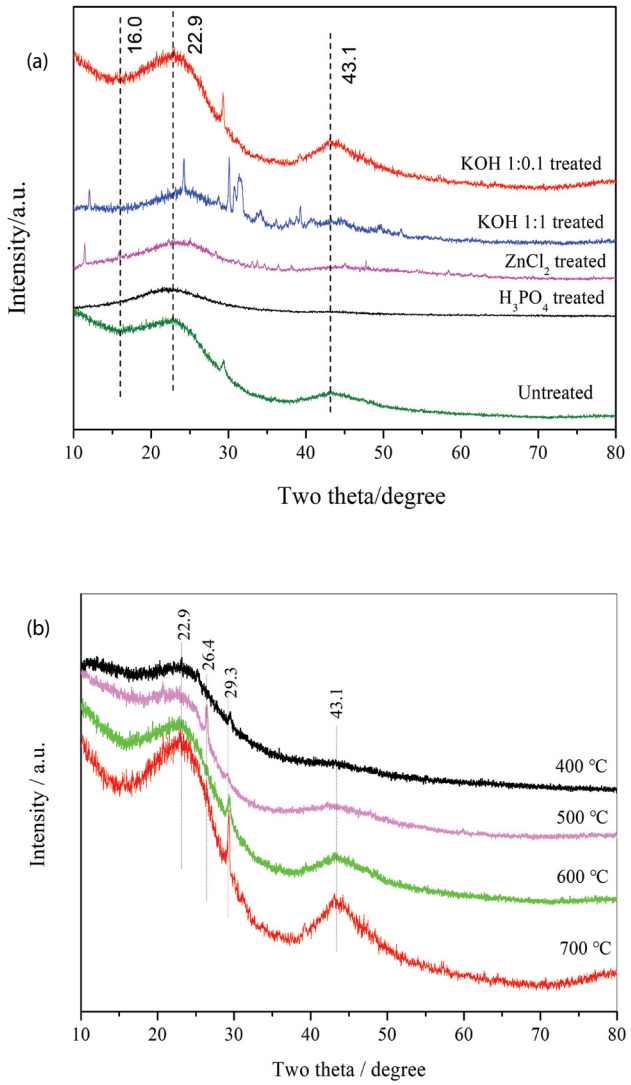

Fig. 1. XRD analysis of WSC (700°C, 2 h) treated by five different chemical activators (a) and WSC treated by KOH (1:0.1) calcined at different temperature (b).

Fig. 1b illustrates the XRD pattern for the WSCs obtained by KOH activator (1:0.1) calcined at different temperature from 400°C to 700°C for 2 h. Compared with Fig. 1a, the intensity of the two peaks 2θ = 22.9° and 43.1° increases with temperature, which indicates that the WSC has been graphitized gradually with calcined temperature. The obvious diffraction peaks at 2θ = 29.3° indicates that the carbonates appeared. During the pyrolysis of biomass raw materials, Ca, Mg, K and other nutrients in biomass carbon are concentrated and enriched. Many researchers believe that increasing the pyrolysis temperature can significantly affect the yield, physical structure and surface properties of biochar. Generally, with the increase of pyrolysis temperature, the yield of biochar will decrease, aromatization will increase, specific surface area and porosity will increase, pH value and adsorption capacity will increase.

3.2. SEM analysis

Fig. 2 shows the surface morphology of WSC (700°C, 2 h) treated by five different chemical activators: untreated WSC (a), WSC treated with ratio of 1:1 to H_3PO_4 (b), $ZnCl_2$ (c), KOH (d), and WSC treated with ratio of 1:0.1 to KOH (e). For untreated sample, it shows that the WSC has an irregular shape of uneven particles with diverse distribution of pores, smooth texture on the surface, fewer pores and smaller pore diameters. The morphology of the modified WSC changed significantly. WSC prepared with H_3PO_4 treated has a compact structure, and its surface structure is damaged and more rough and uneven, showing irregular blocks, and some pores are blocked. WSC (treated with $ZnCl_2$) has a honeycomb pore structure and well-developed pores, indicating that $ZnCl_2$ has a pore-forming effect in the modification of walnut shells. The WSC treated with KOH (1:1) has many irregular and complex pore structures distributed on the surface of the WSC due to the etching effect of strong alkali. Also, the amount of KOH for activation influenced the surface morphology and structure of activated WSC. The noticeable impact of KOH amount on surface can be observed by SEM images of WSC. And the WSC treated with KOH (1:0.1) exhibits a layered two-dimensional structure, and many pores are existed. According to XRD date, this maybe graphic

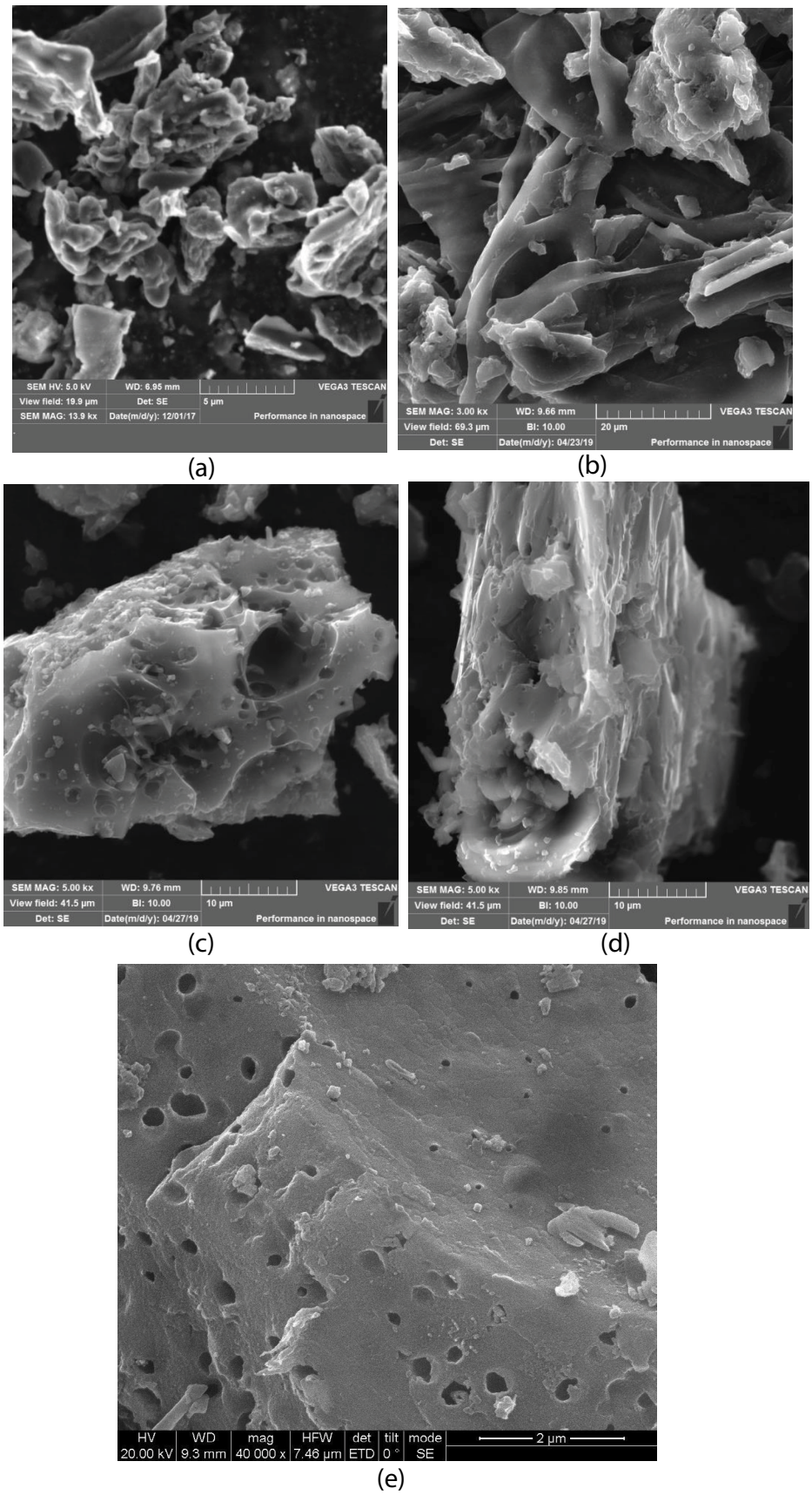

Fig. 2. SEM image of WSC treated with (a) untreated, (b) H_3PO_4, (c) $ZnCl_2$, (d) 1:1 KOH, and (e) 1:0.1 KOH) calcined at 700°C for 2 h.

crystalline formed. Moreover, the irregular intercellular spaces and pores indicated that the glycosidic linkage in hemicellulose and cellulose were hydrolyzed by KOH or H_3PO_4 along with the cleavage of aryl bond in lignin [20,21].

3.3. BET analysis

The adsorption and desorption nitrogen curves of the WSC prepared though different chemical activators are shown in Fig. 3. From Fig. 3 we can see that they have a hybrid shape between Type I and Type IV isotherms. According to the International Union of Pure and Applied Chemistry (IUPAC) nomenclature, it is also seen that the adsorption capacity of the WSC significantly differ from activation method, and the WSC prepared by KOH (1:0.1) has the largest N_2 adsorption capacity, providing a potential adsorbent material with excellent pollutant adsorption ability. The pore morphology parameters of WSC samples including specific surface area, pore volume, pore size and the carbon yield were given in Table 1. It can be seen that the BET surface area for WSC treated by KOH (1:0.1), KOH (1:1), H_3PO_4, $ZnCl_2$ is 435.98, 81.94, 269.18 and 16.85 $m^2\ g^{-1}$, respectively. The total pore volume of WSC treated by the four chemical activators is equal to 0.299, 0.0614, 0.174 and 0.034 $cm^3\ g^{-1}$, respectively. Also the WSC treated as KOH (1:0.1) has the higher carbon yield than KOH (1:1). The pore volume and BET surface of WSC treated by KOH (1:0.1) are higher than KOH (1:1), which is respected for its higher adsorption activity.

3.4. FTIR analysis

The FTIR spectra of the four WSCs treated by different chemical activators are shown in Fig. 4. The absorption peaks around 3,462 cm^{-1} for KOH treated is related to the –OH stretching vibration associated with the hydrogen-bonded hydroxyl group. The moderate absorption peaks at 1,450 cm^{-1} for KOH or H_3PO_4 treated can be assigned to the C–C stretching vibrations in the aromatic rings. And peaks at 1,573 and 1,633 cm^{-1} can be attributed to the C–C and C=C stretching vibrations in the aromatic rings, respectively. The predominant peaks in the range of 1,000–1,127 cm^{-1} of the four WSCs indicate the C–O stretching vibration of the ether groups. The observed peaks at 885 cm^{-1} can be assigned to the out-of-plane bending vibration of =C–H bond in the aromatic rings. Comparing the FTIR spectra of the four WSCs, the WSC treated with KOH (1:0.1) exhibits the higher intensity of the absorption peaks associated with the C–O bond and –OH stretching vibration, which mightbe induced its high phenol adsorption. As reused material of WSC treated with KOH (1:0.1), FTIR spectra shows that peak at 3,462 cm^{-1} intensity becomes larger, and the stronger –OH peak indicates that –OH on WSC and O atom of phenol to

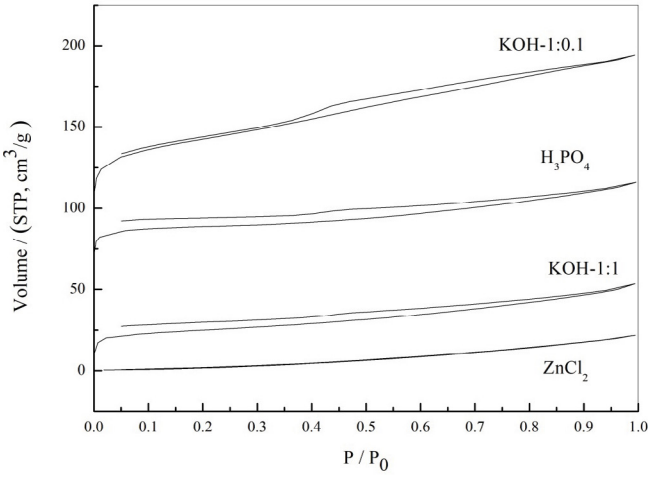

Fig. 3. N_2 adsorption–desorption curves of WSC treated with different activators.

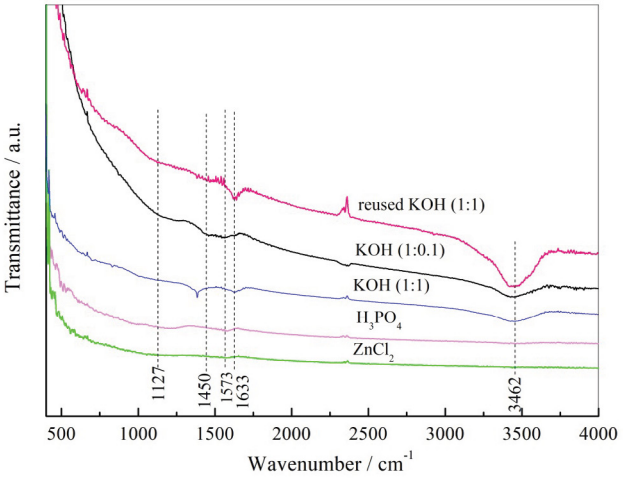

Fig. 4. FTIR spectra of WSC treated with different activators and reused WSC (KOH 1:0.1).

Table 1
Data of surface area, pore volume and mean pore diameter of the samples

Samples	Surface area ($m^2\ g^{-1}$)	Total pore volume ($cm^3\ g^{-1}$)	A_{mes} ($m^2\ g^{-1}$)	A_{mic} ($m^2\ g^{-1}$)	V_{mic} ($cm^3\ g^{-1}$)	D_c (nm)	Yields (%)
H_3PO_4 treated WSC (1:1)	269.2	0.174	27.84	241.3	0.125	2.58	56.7
KOH treated WSC (1:1)	81.9	0.0614	45.58	36.4	0.0188	3.71	36.5
KOH treated WSC (1:0.1)	436.0	0.299	294.64	141.3	0.159	2.75	50.3
$ZnCl_2$ treated WSC (1:1)	16.9	0.034	16.8	0	0	7.15	45.7

form hydrogen bond. At the same time, there is an infrared absorption peak at 1,633 cm^{-1}, which belongs to the absorption peak of C=C bond on the framework of benzene ring. Phenol contains the structure of benzene ring, which proves that phenol is adsorbed on carbon materials. Based on the results, –OH formed and benzene ring adsorption are the key role of the phenol adsorption on the WSC.

3.5. Adsorption of phenol

3.5.1. Effect of treated chemical activators

Fig. 5 shows the phenol adsorption performance of WSC treated with different chemical activators. As can be seen in Fig. 5, the adsorption rate of WSC to phenol all presents a rapid adsorption first and then gradually stable to reach adsorption equilibrium. For 20 mg L^{-1} phenol, the adsorption rate of untreated WSC can reach 89% adsorption efficiency in 60 min. The activity of H_2O treatment and KOH treatment of WSC are higher than untreated, and the adsorption rate in 60 min is 92.23% and 96.46%, respectively. For the chemical activation reagent enters the WSC during the impregnation process, and evaporates from the WSC during the high-temperature activation process. This process formed pores on the surface of the WSC and increased the adsorption performance. From the SEM image, it can be seen that the WSC pretreated by H_3PO_4 presents a block structure, which causes the pores of the WSC to be blocked, and decreased its adsorption efficiency, the adsorption rate in 60 min is 90.57%. Some micropores and mesopores of walnut shell charcoal activated by $ZnCl_2$ were blocked. The existing macropores were not conducive to the phenol adsorption by WSC, and the adsorption rate was 72.31% in 60 min. Strong alkali has an etching effect on WSC, results in a layered structure of WSC and improves activity. In addition, KOH can react with carbon to produce gas under high temperature conditions. When the gas is released, new pores will be created and the activity will increase. The reaction equation is $6KOH + 2C \rightarrow 2K + 3H_2 + 2K_2CO_3$ [22]. In summary, the WSC treated with KOH (1:0.1) has the best phenol adsorption performance.

3.5.2. Effect of different ratios of KOH-treated WSC on phenol adsorption

To study the influence of ratio of walnut shell and KOH on the adsorption capacity of WSC for phenol, experiments were performed at room temperature and phenol initial concentration of 20 mg L^{-1}, changing from 1:0.1 to 1:1.5. Fig. 6a shows the influence curve of the phenol adsorption performance of WSC treated with KOH as different ratios. From Fig. 6a it can be seen that the adsorption rates of WSC are similar along the reaction time. The phenol adsorption rate increases rapidly in the first 10 min, and then the adsorption rate curves gradually separate and tend to parallel. Ratios of KOH have a significant effect on the phenol adsorption performance of WSC. The activity of WSC treated with KOH with mass ratio of 1:0.75 and 1:1.5 at

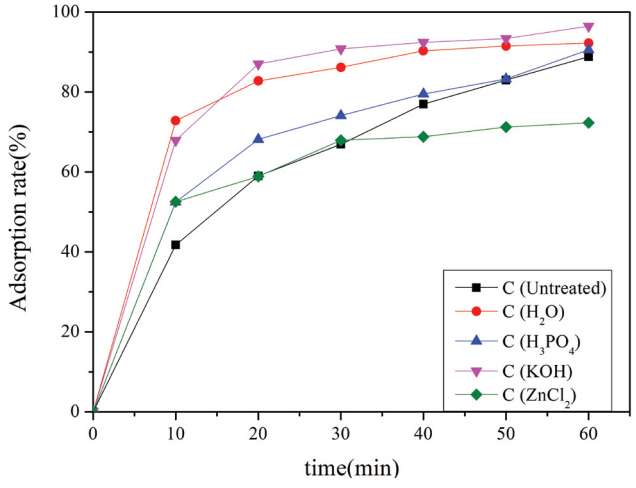

Fig. 5. Adsorption of phenol on WSC treated with different chemical activators (Reaction conditions: 20°C ± 1°C, 20 mg L^{-1} phenol, 2 g L^{-1} dose of WSC, 100 mL solution and pH = 5).

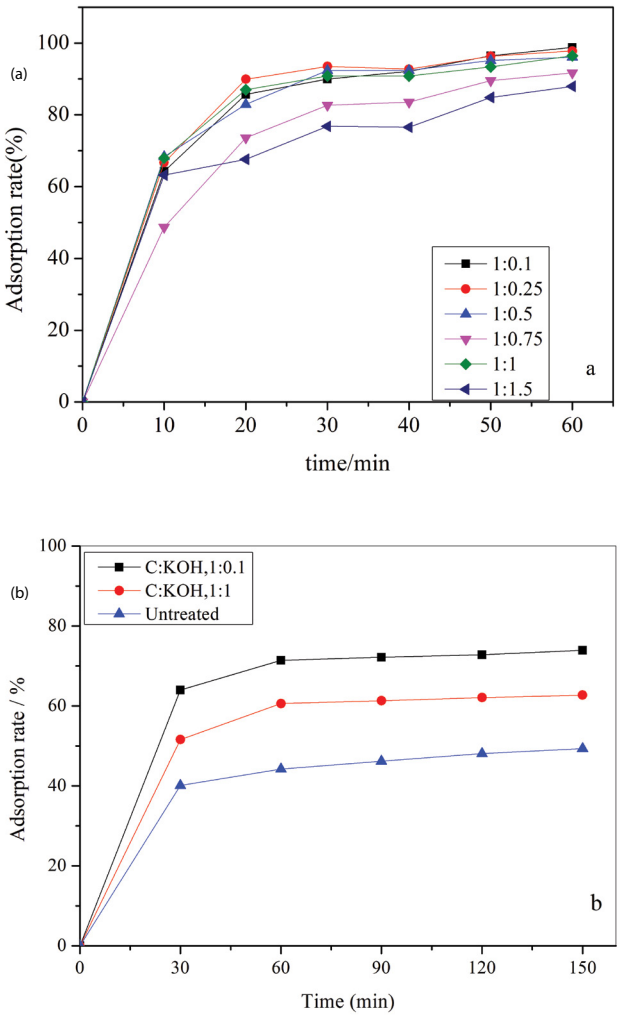

Fig. 6. Phenol adsorption on WSC treated with different KOH ratios (Reaction conditions: 20°C ± 1°C, 20 mg L^{-1} (a) and 80 mg L^{-1} (b) phenol, 2 g L^{-1} dose of WSC, 100 mL solution and pH = 5).

60 min was lower than other ratios, which were 91.68% and 87.95%, respectively. However, if the mass ratio is excessively increased, the micropores will be widened into mesopores or even macropores. After a certain value, the pore walls will be etched due to excessive activation reaction, the specific surface area will be greatly reduced, and the adsorption value will decrease instead. The same conclusion can be obtained from the SEM image. The KOH-treated WSC with a mass ratio of 1:0.1 and 1:0.25 has little difference in activity, and the 60 min adsorption rate is 98.79% and 97.79%, respectively. Therefore, from the perspective of resource conservation and equipment corrosion, the mass ratio of KOH is selected as 1:0.1 activated WSC for subsequent research.

From Fig. 6a, it is little difference for WSC treated with 1:1 and 1:0.1 for phenol adsorption with its concentration of 20 mg L^{-1}. But when phenol concentration increased to 80 mg L^{-1}, it is different obviously (Fig. 6b). KOH treated walnut shell is better adsorption efficiency than untreated, and the KOH ratio is 1:0.1 is better than 1:1.

3.5.3. Effect of calcined temperature

The effect of calcined temperature of WSC on phenol adsorption was investigated by adding 0.2 g into 100 mL 100 mg L^{-1} aqueous solution (Fig. 7). With increasing calcined temperature of WSC from 400 to 700°C, the phenol removal efficiency increased with calcined temperature. For 20 mg L^{-1} of phenol, the adsorption activity of WSC calcined at 400°C is 32.76% in 60 min, while increased to 700°C, the activity reaches 65% in 10 min and then exceeds 95% within 60 min. If continue to increase the calcined temperature of WSC to increase its activity, it is too wasteful of energy and little significance. Therefore, subsequent experiments used WSC roasted at 700°C for research.

3.5.4. Effect of initial phenol concentration

Fig. 8 depicts the effect of initial concentration on the phenol removal from 10 to 300 mg L^{-1}. The adsorption saturation curves rise sharply in the first 10 min, indicating that there are plenty of readily accessible sites. And then, a plateau is reached in all curves indicating that the adsorbent is saturated at this level. It can be seen from Fig. 8 that the initial concentrations of 10–300 mg L^{-1} to reach equilibrium was 20 min. It was also seen that an increase in initial phenol concentration resulted in increased phenol adsorption. The removal curves are single, smooth and continuous, indicating the formation of monolayer coverage of the phenol molecules onto the outer surface of the adsorbent. The adsorption capacity at equilibrium (q_e) increased from 4.80 to 34.60 mg g^{-1} with an increase in the initial phenol concentrations from 10 to 100 mg L^{-1}. For 10 mg L^{-1} phenol solution, the adsorption rate of WSC was 96.49% within 60 min, and for 100 mg L^{-1} is 69.20%. It is because the adsorption capacity of WSC is limited. The higher concentration of phenol solution, the more likely is to reach saturation [23]. And also increases phenol concentration to 300 mg L^{-1}, the phenol adsorption capacity increases to 53.67 mg g^{-1}, and the phenol degradation rate decreases to 35.78%. It can be seen that the adsorption capacity of walnut shell carbon for phenol gradually increases with the initial concentration, but the degradation rate gradually decreases. For the certain amount of walnut shell carbon, the adsorption sites are limited and reach saturated adsorption to a certain extent, which restricts the smooth progress of the adsorption process and reduces the removal rate. Increasing phenol concentration is an impact increasing the capacity of the fixed amount of adsorbent. It indicates that the WSC can be used in phenol concentration lower than 300 mg L^{-1}.

3.5.5. Effect of different pH on phenol adsorption by WSC

The initial pH is an important factor affecting the adsorption capacity of adsorbent, which is attributed to the change of the adsorbent surface with the change in pH value. The experiments were performed in the initial pH range of 3.0–11.0. The influence of pH on the adsorption behavior of WSC for phenol is presented in Fig. 9. It can be

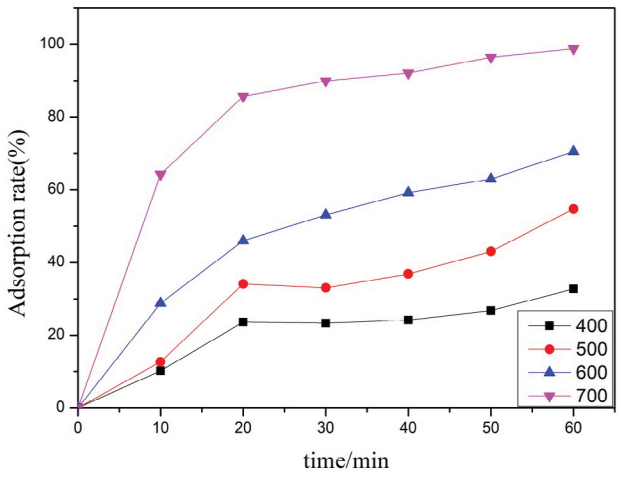

Fig. 7. Adsorption of phenol over WSC at different calcined temperatures (Reaction conditions: 20°C ± 1°C, 100 mg L^{-1} phenol, 2 g L^{-1} dose of WSC, 100 mL solution and pH = 5).

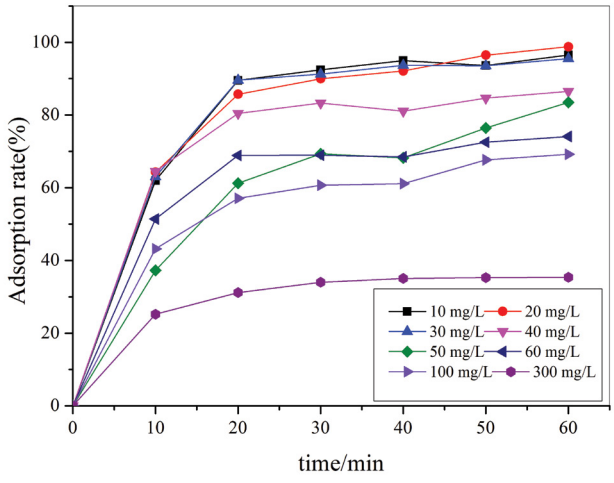

Fig. 8. Adsorption of different concentrations of phenol by WSC (Reaction conditions: 20°C ± 1°C, 10–300 mg L^{-1} phenol, 2 g L^{-1} dose of WSC, 100 mL solution and pH = 5).

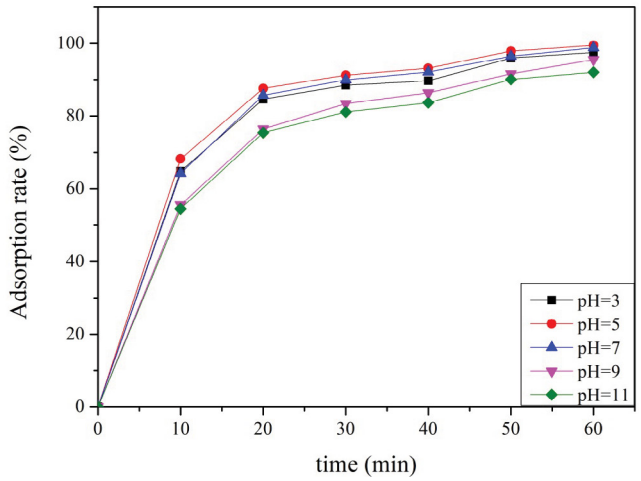

Fig. 9.Adsorption of phenol by WSC at different pH values (Reaction conditions: 20°C ± 1°C, 20 mg L^{-1} phenol, 2 g L^{-1} dose of WSC, 100 mL solution and pH = 5).

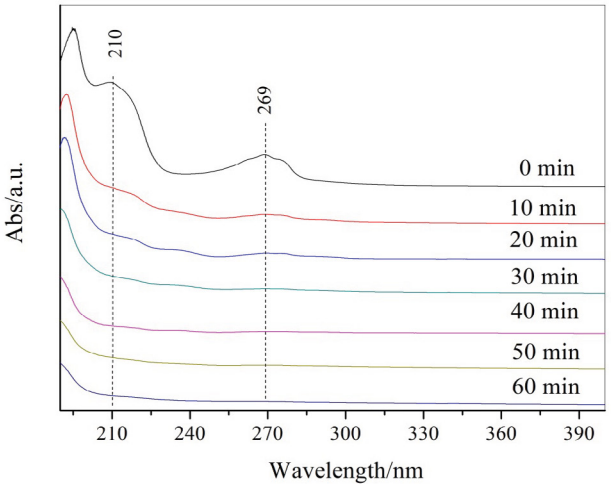

Fig. 10. UV-Vis spectra of phenol adsorption on WSC (Reaction conditions: 20°C ± 1°C, 20 mg L^{-1} phenol, 2 g L^{-1} dose of WSC, 100 mL solution and pH = 5).

seen that the phenol removal efficiency of WSC at pH = 7 is 98.79%, and the highest of pH = 5 is 99.46%, and also the lowest of pH = 11 is 92.05%. This is mainly because phenol is weakly acidic and mainly exists in a molecular state in acidic solutions. At this time, the surface affinity of phenol and WSC is greater than that of water, which is conducive to adsorption. In alkaline solution, phenol is mainly ionized. The existence of the state increases the affinity with water and is not conducive to adsorption. In general, the adsorption capacity of the phenol in the molecular state is larger than that in the ion state, the adsorption rate is best when the pH = 5. In addition, the adsorption rate of the different pH conditions all exceeded 90% at 60 min. This indicates that the pH of the solution has little effect on the adsorption of phenol by the WSC. It shows that the prepared WSC for phenol adsorption has universal applicability.

3.6. UV-Vis spectra

Fig. 10 shows a UV-Vis spectrum of phenol adsorption on WSC prepared under optimal conditions. Fig. 10 suggests that peaks at 210 nm and 269 nm are the characteristic absorption peaks of the E2 and B bands of phenol, respectively. As the adsorption reaction progresses, the characteristic peaks of the phenol become smaller gradually. And at 10–30 min, there is an adsorption peak at 237 nm, which is attributed to p-benzoquinone, which means that phenol adsorbed on WSC with physical adsorption and chemical adsorption. At 60 min, the characteristic peaks were very weak, indicating that there is almost no phenol in the solution at this time, which confirms that the WSC has a good adsorption effect on phenol.

3.7. Adsorption kinetics

The relation between the phenol concentration in the solution at equilibrium (C_e), and the amount of phenol adsorbed on the adsorbent (q_e) is examined by adsorption isotherms. In this study, the equilibrium established between phenol

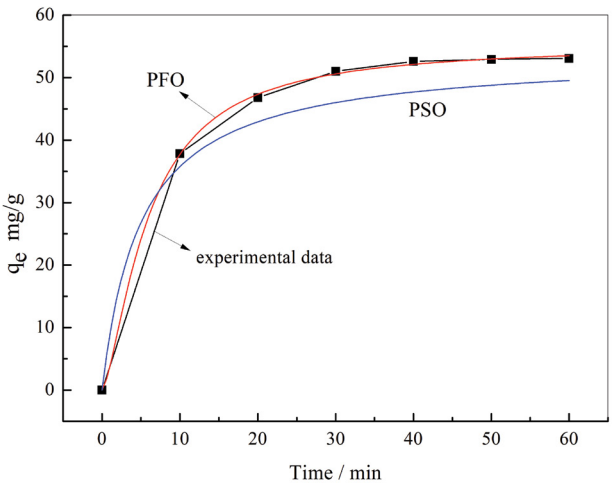

Fig. 11. Experimental data and the fitted non-linear forms of pseudo-first-order equations and pseudo-second-order equations for phenol adsorption on WSC.

and WSC in aqueous solution was described by the non-linear pseudo-first-order and pseudo-second-order models of kinetic equations and its formulas are presented in Table 2 and in Fig. 11. Additionally, the equations have also been used in some literatures [24] for non-linear regression. From the Fig. 11, it is observed that the non-linear pseudo-first-order equations exhibits higher R^2 = 0.9982 values than the non-linear pseudo-second-order equations which R^2 is 0.6715, which considers that the non-linear pseudo-first-order equations better match the phenol adsorption on WSC. On the other hand, the non-linear pseudo-first-order and pseudo-second-order equations have different kinetic parameters from each other. The q_e values of the non-linear pseudo-first-order and pseudo-second-order equations is 53.67 mg g^{-1}. and Table 2 suggests that these values are the best-fit for the experimental data.

Table 2
Non-linear forms of pseudo-first-order and pseudo-second-order equations kinetic model equation plot linear pseudo-first-order

Kinetic model	Plot	
Non-linear pseudo-first-order		
Function: $q_t = q_e (1-e^{-k1t})$	$k_1 = 0.12$ min^{-1}	$R^2 = 0.9982$
Non-linear pseudo-second-order		
Function: $q_t = \frac{k_2 q_e^2 t}{1 + k_2 q_e t}$	$k_2 = 3.73 \times 10^{-3}$ (g mg^{-1} min^{-1})	$R^2 = 0.6715$

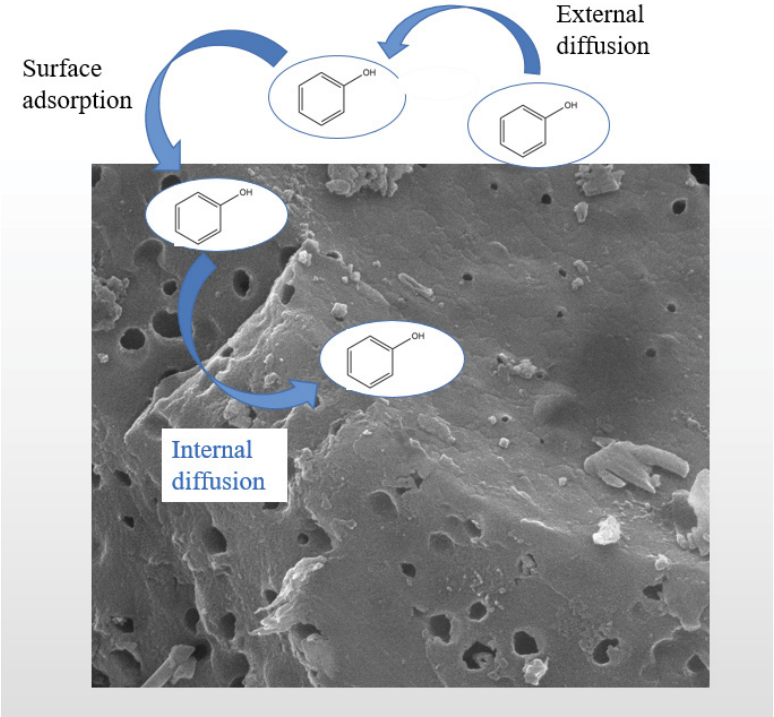

Fig. 12. Proposed mechanism for adsorption of phenol on WSC.

3.8. Proposed adsorption mechanism

In conclusion, based on the phenol molecule structure and the chemical functions present on the surface of WSC (Fig. 12), the adsorption of phenol by WSC mainly depends on the external diffusion speed, that is, the faster the relative movement speed of WSC and phenol, the higher the adsorption efficiency. The first reaction between walnut shell carbon and phenol in solution is surface adsorption. The phenol adsorbed on the surface of walnut shell carbon will further diffuse into walnut shell carbon through internal diffusion. The adsorbed phenol still exists in the form of molecule state [25].

4. Conclusions

This work investigate the application of the KOH-treated walnut shell to prepare WSC and used for the phenol adsorption from water. The interactive effects of the operating parameters (pH, initial concentration and adsorbent dosage) on phenol removal were studied. The produced WSC were characterized by BET, SEM, FTIR and XRD analyses. The surface morphology study and other characterization results showed that the surface area and the porous structure of the WSC can obtain at 700°C. The experimental conditions were found to be pH = 5, initial concentration is 20 mg L^{-1}, adsorbent dosage is 0.20 g and contact time is 60 min. The WSC calcined at 700°C suggested the highest removal efficiency (98.79%) at the optimized conditions compared to other biochars. The BET specific surface area was 435.98 m^2 g^{-1}, and the pore volume was 0.299 cm^3 g^{-1}, indicating that the WSC was mesoporous structure. In addition, the experimental results show that the adsorption temperature and pH has little effect on the phenol adsorption on WSC. The kinetic study shows that the phenol adsorption on WSC fits the non-linear pseudo-first-order. It suggests that the phenol adsorption on WSC is accompanied by mainly physical adsorption.

This work presented the potential of the recycled walnut shell for production of a low cost and a high-quality biochar for phenol adsorption application.

Acknowledgement

The present study was supported by the Yunnan Provincial Agricultural Joint Project (No. 2018FG001-051), Yunnan Provincial Department of Education Research Fund (No. 2020Y0414) and Key Laboratory of State Forestry and Grassland Administration on Highly-Efficient Utilization of Forestry Biomass Resources in Southwest China (No. 2021-KF02).

References

[1] Y. Ma, N. Gao, W. Chu, C. Li, Removal of phenol by powdered activated carbon adsorption, Front. Environ. Sci. Eng. China, 7 (2013) 158–165.
[2] B.H. Hameed, A.A. Rahman, Removal of phenol from aqueous solutions by adsorption onto activated carbon prepared from biomass material, J. Hazard. Mater., 160 (2008) 576–581.
[3] Z. Wang, D. Shen, C. Wu, S. Gu, State-of-the-art on the production and application of carbon nanomaterials from biomass, Green Chem., **20** (2018) 5031–5057.
[4] Y. Gokce, Z. Aktas, Nitric acid modification of activated carbon produced from waste tea and adsorption of methylene blue and phenol, Appl. Surf. Sci., 313 (2014) 352–359.
[5] T.K.M. Prashanthakumar, S.K. Ashok Kumar, S.K. Sahoo, A quick removal of toxic phenolic compounds using porous carbon prepared from renewable biomass coconut spathe and exploration of new source for porous carbon materials, J. Environ. Chem. Eng., 6 (2018) 1434–1442.
[6] D. Chen, K. Kannan, H. Tan, Z. Zheng, Y.-L. Feng, Y. Wu, M. Widelka, Bisphenol analogues other than BPA: environmental occurrence, human Exposure, and toxicity–a review, Environ. Sci. Technol., 50 (2016) 5438–5453.
[7] A.B. Fuertes, M. Sevilla, High-surface area carbons from renewable sources with a bimodal micro-mesoporosity for high-performance ionic liquid-based supercapacitors, Carbon, 94 (2015) 41–52.
[8] Y. Li, G. Wang, T. Wei, Z. Fan, P. Yan, Nitrogen and sulfur co-doped porous carbon nanosheets derived from willow catkin for supercapacitors, Nano Energy, 19 (2016) 165–175.
[9] J. Serafin, M. Baca, M. Biegun, E. Mijowska, R.J. Kaleńczuk, J. Sreńscek-Nazzal, B. Michalkiewicz, Direct conversion of biomass to nanoporous activated biocarbons for high CO_2 adsorption and supercapacitor applications, Appl. Surf. Sci., 497 (2019) 143722, doi: 10.1016/j.apsusc.2019.143722.
[10] N.A.S. Mohammed, R.A. Abu-Zurayk, I. Hamadneh, A.H. Al-Dujaili, Phenol adsorption on biochar prepared from the pine fruit shells: equilibrium, kinetic and thermodynamics studies, J. Environ. Manage., 226 (2018) 377–385.
[11] A. Ould-Idriss, M. Stitou, E.M. Cuerda-correa, C. Fernández-González, A. Macías-García, M. Alexandre-Franco, V. Gómez-Serrano, Preparation of activated carbons from olive-tree wood revisited. I. Chemical activation with H_3PO_4, Fuel Process. Technol., 92 (2011) 261–265.
[12] C. Namasivayam, D. Sangeetha, Equilibrium and kinetic studies of adsorption of phosphate onto $ZnCl_2$ activated coir pith carbon, J. Colloid Interface Sci., 280 (2004) 359–365.
[13] D. Duranoğlu, Ü. Beker, Steam and KOH activated carbons from peach stones, Energy Sources Part A, 34 (2012) 1004–1015.
[14] G. Duman, Y. Onal, C. Okutucu, S. Onenc, J. Yanik, Production of activated carbon from pine cone and evaluation of its physical, chemical, and adsorption properties, Energy Fuels, 23 (2009) 2197–2204.
[15] B.M.V. da Gama, G. Nascimento, D.C.S. Sales, J.M. Rodríguez-Díaz, C.M.B. de Menezes Barbosa, M.M.M.B. Duarte, Mono and binary component adsorption of phenol and cadmium using adsorbent derived from peanut shells, J. Cleaner Prod., 201 (2018) 219–228.
[16] X. Ma, L. Li, R. Chen, C. Wang, K. Zhou, H. Li, Porous carbon materials based on biomass for acetone adsorption: effect of surface chemistry and porous structure, Appl. Surf. Sci., 459 (2018) 657–664.
[17] Z.-j. Yi, J. Yao, Y.-f. Kuang, H.-l. Chen, F. Wang, Z.-m. Yuan, Removal of Pb(II) by adsorption onto Chinese walnut shell activated carbon, Water Sci. Technol., 72 (2015) 983–989.
[18] H. Zhao, Q. Yu, M. Li, S. Sun, Preparation and water vapor adsorption of "green" walnut-shell activated carbon by CO_2 physical activation, Adsorpt. Sci. Technol., 38 (2020) 60–76.
[19] Y. Luo, D. Li, Y. Chen, X. Sun, Q. Cao, X. Liu, The performance of phosphoric acid in the preparation of activated carbon-containing phosphorus species from rice husk residue, J. Mater. Sci., 54 (2019) 5008–5021.
[20] A.S. Azis, M. Hashim, N.M. Saiden, N. Daud, N.M.M. Shahrani, Study the iron environments of the steel waste product and its possible potential applications in ferrites, Adv. Mater. Res., 1109 (2015) 295–299.
[21] M.S. Shamsuddin, N.R.N. Yusoff, M.A. Sulaiman, Synthesis and characterization of activated carbon produced from Kenaf Core Fiber using H_3PO_4 activation, Procedia Chem., 19 (2016) 558–565.
[22] L. Muniandy, F. Adam, A.R. Mohamed, E.-P. Ng, The synthesis and characterization of high purity mixed microporous/mesoporous activated carbon from rice husk using chemical activation with NaOH and KOH, Microporous Mesoporous Mater., 197 (2014) 316–323.
[23] U. Beker, B. Ganbold, H. Dertli, D.D. Gülbayir, Adsorption of phenol by activated carbon: influence of activation methods and solution pH, Energy Convers. Manage., 51 (2010) 235–240.
[24] M. Khalid, G. Joly, A. Renaud, P. Magnoux, Removal of phenol from water by adsorption using zeolites, Ind. Eng. Chem. Res., 43 (2004) 5275–5280.
[25] M. Ur Rehman, A. Manan, M. Uzair, A.S. Khan, A. Ullah, A.S. Ahmad, A.H. Wazir, I. Qazi, M.A. Khan, Physicochemical characterization of Pakistani clay for adsorption of methylene blue: kinetic, isotherm and thermodynamic study, Mater. Chem. Phys., 269 (2021) 124722, doi: 10.1016/j.matchemphys.2021.124722.